

A NOVEL TUNING TECHNIQUE OF MULTI-BAND POWER SYSTEM STABILIZER USING EXPECTATION AND MAXIMIZATION ALGORITHM FOR MULTI-MACHINE SYSTEM

A.RAGAVENDIRAN
Pondicherry Engineering college
Department of EEE
Pillaichavady, Puducherry
India
ragavendiran.as@gmail.com

R. GNANADASS
Pondicherry Engineering college
Department of EEE
Pillaichavady, Puducherry
India
gnanadass@pec.edu

M.KAVITHA
Dr SJSPM College of Engg& Tech.
Department of EEE
Pathukannu, Puducherry
India
kavithamrgn@gmail.com

Abstract: Generators have to meet the change in real and reactive power demand of the practical power system. The real power variations in the system have to meet out by the rescheduling process of the generators. But there is a huge trust to meet out the reactive power load demand. The excitation loop of the corresponding generator is adjusted with its electric limits to activate the reactive power of the network. To expedite the reactive power delivery, multi band power system stabilizer (MB-PSS) is connected in the exciter loop of the generator for various system conditions. In this paper, a new Sparse Recursive Least Square (SPARLS) algorithm is demonstrated to tune the MB-PSS parameters to meet the vulnerable conditions. The proposed SPARLS algorithm makes use of expectation maximization (EM) algorithm to tune the MB-PSS. A comparative study between the proposed SPARLS and RLS algorithm has been performed on three machine nine bus systems. The simulation results obtained will validate the effectiveness of the proposed algorithm and the impact of stability studies of the power system operation under disturbances. The SPARLS algorithm is also used to tune the parameters of MB-PSS to achieve quicker settling time for the system parameter such as load angle, field voltage and speed deviation. It is found that the SPARLS is a better algorithm for the determination of optimum stabilizer parameter.

Key-Words: Power system stabilizer, PID controller, RLS algorithm, SPARLS algorithm, SMIB system, EM method

1 Introduction

In a power system, low frequency oscillation is one of the most important phenomena that occur in a dynamical system. Damped oscillations are contributing an important role in power system. These oscillations will damp automatically after particular time because both AVR and generator field coil will produce some amount of damping torque. If oscillations are not properly controlled, it will damage the system and the relay pick will block out the generator from the system. In order to, avoid the above mentioned problems, the power system stabilizers are widely used to damp out the oscillation of the electrical machines in the power system. Larsen et al. designed the PSS based linear model of the plant using a particular operating point [1]. However, almost all the power systems are nonlinear and the operating point is changeable, which changes with respect to the operating condition. Therefore, the performance of a Conventional

Power System Stabilizer (CPSS) may deteriorate under variations that result from nonlinear and time-varying characteristics of the controlled plant. The PSS performance is highly sensitive to wide range operating point when artificial intelligence approaches and fuzzy logic are used to tune the PSS [2-4]. Similarly, artificial neural networks [5] and Neuro-fuzzy based PSS have been presented to tune the PSS in [6-7]. The application of robust control methods for designing PSS has been presented in [8-10] and adaptive control algorithms based PSS are presented in [11-13]. Most of the adaptive PSS proposed so far have the signal-synthesizing problem with self-tuning controller. A self-tuning PID excitation controller is proposed in this paper to improve the damping of a synchronous machine. Tabatabaei et al. proposed a comparative study to analyze the performance of PI and PID controller [14], and from the analyze, the author has demonstrated that the PID controller is giving better dynamic response than a PI controller. To tune

the PID, various self-tuning methods have been proposed, such as Particle swarm optimization, Genetic algorithm, Fuzzy logic and pole placement nonlinear programming techniques [15-17]. The recursive fuzzy identification approach is used to tune the PSS for a complex nonlinear system as in [18]. The recursive least square (RLS) and genetic algorithm are used together to tune the PID controller. The RLS developed to estimate the system parameters. The genetic algorithm (GN) is developed to tune the system parameters. Both RLS and GN algorithms are established in the ladder programming environment [19]. The above mentioned methods are computationally complex and the solution requires a large number of iterations. In general, the RLS algorithm cannot force any limits on the input parameter formation. As an effect of this simplification, the computation complexity is $O(n^3)$ per time iteration (where n is the size of the data matrix). This becomes the major drawback for their applications as well as for their cost effective implementation. Therefore, to tune the PSS in an interconnected system, less complexity with less iteration is required. When comparing the above mentioned drawback method with RLS technique, it is less iteration with the fast converging method but computationally complex one. The Sparse RLS algorithm is compared with the RLS, a technique which is less computational complexity and fast converging. The sparse vectors require less time to converge [20 & 21]. In this paper, three machine nine bus system and power system stabilizer have been modelled using Simulink block sets. The performance of the MB-PSS and PID has been demonstrated on the three machine nine bus systems. The characteristic behavior of the conventional RLS is compared with SPARLS when subjected to different case studies on the above test system. The outline of the paper is as follows: First section describes the necessity of MB-PSS and detailed state of the art about its performance. Section 2 describes the optimization of the MB-PSS and PID controller structures. The brief background of the SPARLS algorithm is given in the Section 3. Section 4 discusses the three machine nine bus systems. Simulation results are provided in the Section 5. Finally, the conclusions are presented in the Section 6.

2 General Block Diagram of Multi Band Power System Stabilizer

The need for effective damping of a wide range of electromechanical oscillations motivated the concept of the MB-PSS. As its name reveals, the MB-PSS structure is based on multiple working bands.

Three separate bands are used with the MB-PSS, respectively dedicated to the low, intermediate, and high frequency modes of oscillations. The low band is typically associated with the power system global mode, the intermediate band with the inter-area modes, and the high band with the local modes. The low band is taking care of very slow oscillating phenomena such as common modes found in an isolated system with a typical frequency range of 0.05 Hz. The intermediate band is used for inter-area modes usually found in the range of 0.2 to 1.0 Hz. The high bands are dealing with local modes, either plant or inter machines, with a typical frequency range of 0.8 to 4.0 Hz. Each of the three bands is made of a different band-pass filter, gain, and limiter as shown Figure 1. The outputs of the three bands are summed and passed through a final limiter producing the stabilizer output V_{stable} (Figure 1). This signal, then modulates the set point of the generator voltage regulator so as to improve the damping of the electromechanical oscillations. Usually, a few of the lead-lag blocks should be used in MB-PSS circuits. The MB-PSS comprises three main functions, the transducers, the lead-lag compensator and the limiters. Two speed deviation transducers are required to feed the three band structure used as lead-lag compensator. Four adjustable limiters are provided, one for each band and one for the total PSS output are shown in Figure 1. Multi-band power system stabilizer simulation diagram is shown in Fig. 2. The speed deviation transducers of MB-PSS is shown in Fig. 2, are both derived from machine terminal voltages and currents. The first one, so called $\Delta\omega_1$, is associated with the first two bands. Its measurement is accurate in the 0 to 2.0 Hz range. $\Delta\omega_2$, the second transducer is designed for the high band with a frequency range of 0.8 to 5.0 Hz. Conventional MB-PSS provides effective damping only on a particular operating point. But MB-PSS cannot damp a wide range operating point. PID based MB-PSS provides good damping for a wide range of operating points. The function of PID controller has been discussed bringing in the next section.

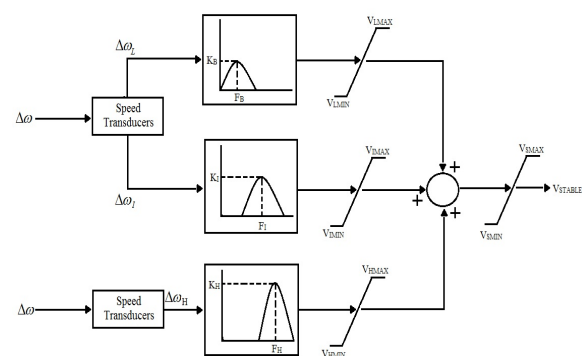


Figure 1: Multiband Power system stabilizer

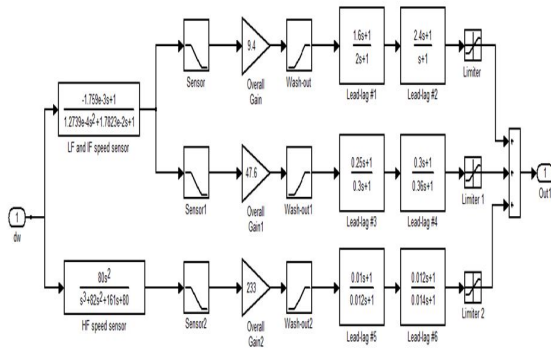


Figure 2: Simulink diagram of multi band power system stabilizer

3 Problem identification

The entire systems are modelled based on linear-time-invariant state-space theory around an operating point from a set of nonlinear differential equations. The linearized system model is represented in terms of the state matrix (A), input matrix (B), output matrix (C), and feed-forward matrix (D) shown in

$$\dot{X} = Ax = By \tag{1}$$

$$Y = Cx + Du \tag{2}$$

where x is the vector of state variables and u is the vector of input variables. The eigenvalues determined from state matrix reflect the overall system stability. Therefore, objective functions are formulated to move eigenvalue forcefully from unstable region (right side of s-plane) to stable region (left side of s-plane). The key properties of an eigenvalue ($\lambda = \sigma \pm j\omega$) are damping factor (σ) and the damping ratio (ξ) that are determined from

$$\sigma_i = \text{real}(\lambda) \tag{3}$$

$$\xi_i = -\frac{\sigma_i}{\sigma_i^2 + \omega_i^2} \tag{4}$$

The main purpose of objective function formulation is to shift eigenvalues from unstable region to stable region. These types of objective functions are formulated by focusing property of eigenvalues (either or) that partially ensure system stability for total operating points. From research paper [16 & 17], the objective function is constructed to improve only damping factor as shown in equation (5). Damping Index (DI) is considered as the objective function that considered

all dominant modes to achieve maximum damping ratios. Here, DI is minimized in order to optimize controller parameters

$$\text{Objective function} = \text{Min}DI = \sum_{i=1}^n (1 - \xi_i) \tag{5}$$

where

ξ = damping ratio

$i = 1, 2, \dots, n$ and n is the total number of eigenvalues in the power system.

The objective functions are maximized or minimized in order to achieve system stability under constraints of damping controller parameters shown

$$K_{stab}^{min} \leq K_{stab} \leq K_{stab}^{max} \tag{6}$$

K_{stab} =stabilizer gain

$$T_1^{min} \leq T_1 \leq T_1^{max} \tag{7}$$

T_1 - Time constant of lead compensator

$$T_2^{min} \leq T_2 \leq T_2^{max} \tag{8}$$

T_1 - Time constant of lead compensator

$$T_w^{min} \leq T_w \leq T_w^{max} \tag{9}$$

T_w Washout Time constant Conventional PSS provides effective damping only on a particular operating point. But PSS cannot damp a wide range operating points. PID based PSS provides good damping for a wide range of operating points. The function of PID controller has been discussed brought in the next section.

4 Proportional Integral and Derivative Controller

A PID controller is a simple three-term controller. The letters P, I and D stand for: P -Proportional, I Integral and D Derivative. The transfer function of the most basic form of PID controller,

$$C(s) = K_p + \frac{K_i}{S} + K_d(s) \tag{10}$$

where

- K_p = Proportional gain,
- K_I = Integral gain and
- K_D =Derivative gain.

The effects of increasing each of the controller parameters K_P , K_I and K_D can be summarized as

- Use K_P to decrease the rise time.
- Use K_D to reduce the overshoot and settling time.
- Use K_I to eliminate the steady-state error.

The self tuning gains of the PID controller [22]

$$K_p = (s_1 + 2s_2)/(1 + r_1) \quad (11)$$

$$K_I = -(s_0 + s_1 + s_2)/T_5 \quad (12)$$

and

$$K_D = [r_1s_1 - (1 - r_1)s_2]/(1 + r_1)T_5 \quad (13)$$

Where s_0, s_1, s_2 , and r_1 are algorithm estimated values [22]. In this paper, self tuning PSS and PID controller are proposed by RLS and SPARLS algorithm. The RLS algorithm is used for automatic tuning of PSS and PID controller. The Recursive Least Square is one of the basic and fast converging methods used for automatic tuning of PSS and PID controller, but computationally this is the complex algorithm.

5 RLS algorithm

The RLS algorithm is used to identify the system parameters and helps to adjust the gains of the PID controller for system stability. The sampling data is generated by executing the system parameters for a specified interval of time. By applying the RLS algorithm, a sampling sequence is formed. The optimal system parameter estimation is carried out by obtaining the mean value of two successive moments of sampling. Fast response when compared to AI techniques. It is used to find out the least mean square error of the system in a recursive manner. RLS used for MB-PSS tuning and to determine the optimal system parameter. Manual calculation is complex. RLS algorithm is using to reduce the Mean Least Square error (MLE). This MLE problem is hard to solve in RLS algorithm. But by using the SPARLS (EM) algorithm, it is easy to solve. SPARLS algorithm slightly modified from RLS algorithm. Schematic difference of the Sparse RLS and RLS algorithm is shown in Fig. 3.

5.1 SPARSE RLS (SPARLS) algorithm

The term sparse refers to a computable property of a vector, x , where x is small in sense but not length that is important. Instead sparsity concerns

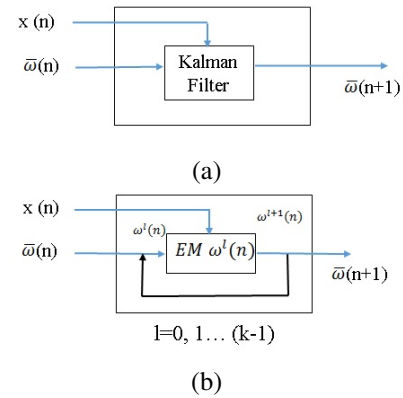


Figure 3: Schematic diagram (a) RLS algorithm (b) SPARLS algorithm

the number of non-zero entries in the vector. A wide range of attractive estimation problem deals with the estimation of sparse vectors. Many values of attention can naturally be modelled as sparse. The SPARLS algorithm is used to identify the system parameters and helps to adjust the gains of the PSS/PID controller to bring the stability of the system. The sampling data is generated by executing the system parameters for a specified interval of time. By applying the SPARLS algorithm, a sampling sequence is formed. The optimal system parameter estimation is carried out by obtaining the mean value of the two successive moments of sampling. The forming and description of the SPARLS sampling is explained as follows: Let the system model (1) is given in the form

$$Ay(m) = Bx(m - 1) \quad (14)$$

where $x(m - 1)$ is a discrete delay input signal, $y(m)$ is discrete output signal, and consider a system described by its input output relationship

$$y(m) = a_1y(m - 1) + a_2y(m - 2) = b_u(m - 1) + b_2u(m - 2) \quad (15)$$

Which is co-efficient estimation by RLS method

$$A(z^{-1})y(z^{-1}) = z^{-1}B(z^{-1})u(z^{-1}) \quad (16)$$

Where z^{-1} is the backward shift operation. The value of the polynomials for the above discrete function is determined as follows:

$$A(z^{-1}) = 1 + a_1z^{-1} + a_2z^{-2} + \dots + a_{na}z^{-na} \quad (17)$$

$$B(z^{-1}) = b_0 + b_1z^{-1} + b_2z^{-2} + \dots + b_{nb}z^{-nb} \quad (18)$$

83 where A and B are polynomials. a_1, \dots, a_{na} and b_0, \dots, b_{nb} are co-efficient of polynomials. A generalized model

of the system (2) can be presented in the following form

$$y(m) = u^T \theta \quad (19)$$

where θ is the unknown parameter and u is the known parameter. The unknown parameters are defined as

$$u^T = [-a_1 \dots -a_{na}, b_0 \dots b_{nb}] \quad (20)$$

This consists of measured values of input and output

$$y^T(m) = [y(m-1) \dots y(m-na), x(m-1) \dots x(m-nb-1)] \quad (21)$$

where An accurate description of the system can be obtained by the model (5). Hence, the system parameters θ should be determined from the output and input of signal samples at the system.

$$y(m) = u^T(m) \hat{\theta} + e(m) \quad (22)$$

where $\hat{\theta}$ is a vector of unknown sampling parameter of the system, and is an error in the modelling. $\hat{\theta}$ should be correctly identified so as to minimize the modeling uncertainties. From the equation 14, the error is obtained as

$$e(m) = x(m) - d(m) \quad (23)$$

The canonical form of the problem typically assumes that the input-output sequences are generated by a time varying system with parameters represented by $w(m)$. Thus the process is described by an estimate of the desired model

$$d(m) = w(m)y(m) + \eta(m) \quad (24)$$

Where $\eta(m)$ is the observation error. $d(m)$ is the desired output of the filter at time. The error will be assumed to be random error. The estimator has only access to the streaming parameter $x(m)$ and $d(m)$. $d(m)$ value is substituted in the error equation (6), the error is obtained as

$$e(m) = x(m) - (w(m)y(m) + \eta(m)) \quad (25)$$

The SPARLS algorithm is associated for updating error coefficients so that the SPARLS algorithm can be operated in an unknown parameters and nonlinear system. The system error characteristic is determined by adjusting system coefficients according to the system parameter conditions and performance criteria assessment. The input vector at time is defined by

$$x(m) = [x(m), x(m-1), \dots, x(m-N-1)]^T \quad (26)$$

The weight vector at time m is defined by

$$w(m) = [w_0(m), w_1(m), \dots, w_{N-1}(m)]^T \quad (27)$$

The operation of the adaptation at time can therefore be stated as the following optimization problem

$$\min_{w(m)} = f(e(1), e(2), \dots, e(m)) \quad (28)$$

Where $f \geq 0$ is a certain cost performance. With an appropriate choice of f , one can possibly obtain a good approximation to $w(m)$ by solving the optimization problem given in above equation. In general, this is an estimation problem. The Lagrangian formulation shows that if $f = f_{rls}$, the optimum solution can be equivalently derived from the following optimization problem

$$\min_{w(m)} \frac{1}{2\sigma^2} |D(m)^{1/2} d(m) - D(m)^{1/2} X(m)w(m)|_2^2 + \gamma(w(m))_1 \quad (29)$$

$$D(m) = \begin{pmatrix} \lambda^{n-1} & \cdot & 0 & 0 \\ \cdot & \lambda^{n-2} & \cdot & 0 \\ 0 & \cdot & 0 & \cdot \\ 0 & 0 & \cdot & 1 \end{pmatrix} \quad (30)$$

Let $x \in C^N$ be a vector in which most of its weight is distributed on a small number of the total set of vectors known as sparse i.e. A vector x is called sparse, if $|x|_0 \ll N$. For any x , let $|x|_0$ denote the number of non-zero coefficients of x . The l_0 quasi-norm of x as follows

$$|w(m)|_0 = \left| \frac{x_n}{x_n} \neq 0 \right| \quad (31)$$

the following cost function

$$f_w(m) = \frac{1}{2\sigma^2} |D(m)^{1/2} d(m) - D(m)^{1/2} X(m)w(m)|_2^2 + \gamma|\hat{w}(m)|_1 \quad (32)$$

$$= \frac{1}{2\sigma^2} |d(m) - X(m)w(m)^* D(m) d(m) W(m)|_2^2 + \gamma|w(m)|_1 \quad (33)$$

The expectation maximization algorithm is an efficient technique for the iterative procedure to compute the maximum likelihood estimate in the presence of missing or hidden data. In each iteration, the EM algorithm consists of two steps i.e. E-step and M-step. The maximum likelihood problem is

$$\max_{w(m)} \left\{ \log p\left(\frac{d(m)}{w(m)}\right) - \gamma|\hat{w}(m)| \right\} \quad (34)$$

This ML problem in general is hard to solve. But by using the EM algorithm, it is easy to solve. The idea is to decompose the error vector $\eta(m)$ in order to divide the optimization problem. The l^{th} iteration of the EM algorithm is as follows

E-step:

$$Q(w|w(m)) = -\frac{1}{2\sigma^2} |r^J - w|_2^2 - \gamma|w|_1 \quad (35)$$

where

$$r^l(m) = (I - \frac{\alpha^2}{\sigma^2} X^*(m)D(m)X(m))\hat{w}(m) + \frac{\alpha^2}{\sigma^2} X^*(m)D(m)d(m) \quad (36)$$

where $\sigma = d(m) - x^{(m)}w(m-1)$ is the a priori error.

M-step:

$$\hat{w}^{l+1}(m) = \text{sign}(r^l(m)) \cdot (|r^l(m)| - \gamma\alpha^2 I) \quad (37)$$

In order to simplify the low complexity implementation of the EM algorithm for $r^l(m) \in R^N$. Generalization of $r^l(m) \in C^N$ is straightforward, since the low complexity implementation can be applied to the real and imaginary parts of $r^l(m)$ independently. Let I^l be the support of $r^l(m)$ at the I^{th} iteration. Let

$$I_{\pm}^{(l)} = \{ir^{(l)}(n) > \gamma\alpha^2 \subset I^{(l)}\} \quad (38)$$

$$w_i^{l+1}(n) = \begin{cases} r_i^l \pm \gamma\alpha^2 & i \in I^{(l)} \\ 0 & i \in I^{(l)} + UI^{(l)} \end{cases} \quad (39)$$

for $i = 1, 2, \dots, N$.

$$B(m) = I - \frac{\alpha^s}{\sigma^2} x^*(m)D(m)x(m) \quad (40)$$

$$u(m) = \frac{\alpha^2}{\sigma^2} x^*(m)D(m)x(m) \quad (41)$$

$$B(m)w^{l+1}(m) = B_{I_{\pm}^{(l)}}^{(l)}(r_{I_{\pm}^{(l)}}^l(n) \pm \gamma\alpha^2 1_{I_{\pm}^{(l)}}) \pm \gamma\alpha^2 1_{I_{\pm}^{(l)}} \pm \gamma\alpha^2 1_{L_{\pm}^{(l)}} \quad (42)$$

This new set of iteration has a lower computational complexity, since it restricts the matrix multiplications to the instantaneous support of the estimate $r^{(l)}(m)$, which is expected to be close to the support of $w(m)$. The above equations denote the iterations of low-complexity expectation maximization algorithm. Upon the arrival of the n^{th} input, $B(m)$ and $u(m)$ can be obtained via the following updated rules

$$B(m) = \lambda B(m-1) - \frac{\alpha^2}{\sigma^2} x(m)d(m) + (1-\lambda)I \quad (43)$$

$$u(m) = \lambda u(m-1) + \frac{\alpha^2}{\sigma^2} x(m)d(m) \quad (44)$$

Upon the arrival of the M input, the SPARLS algorithm computes the estimate $w^{(l)}(m)$ i.e. update the $w^{(l+1)}(m)$ by given $B(m)$ and $u(m)$. The input arguments are the number of EM iterations. Without loss of generality, it can set the time index $\eta = 1$ such

that $x(1) \neq 0$. The main objective of SPARLS error cancellation is accomplished by feeding the system output back to the SPARLS algorithm and adjusting the controller through a SPARLS algorithm to minimize the number of input samples, better peak signal to error ratio and convergence time. SPARLS algorithms have the ability to adjust its impulse response to algorithm to find out the correlated signal in the input. It requires the knowledge of the signal and error characteristics. SPARLS algorithms have the capability of SPARLS tracking the signal under non-stationary conditions. Error cancellation is a variation of optimal algorithm that involves producing an estimate of the error by algorithm the reference input and then subtracting this error estimate from the primary input containing both system response and error. The flow chart of SPARLS algorithm is given below

5.2 Steps by Step Procedure for SPARLS Algorithm

Step 1. Initialize the reference parameter such as MB-PSS parameters.

Step 2. Run the system obtain sample values.

Step 3. Calculate the output $y(m)$ from obtaining parameters using equation (16).

step 4. The proposed algorithm is an estimation of sparse vectors (26).

Step 5. Estimate error between set value and the desired value.

Step 6. Update the error using equation (34).

Step 7. Calculate the value of MB-PSS parameter.

Step 8. Update the new MB-PSS parameter.

6 System Description

The demonstrated test system consists of three generators, nine buses, six numbers of 230 KV transmission line, three transformers, 315 MW, 115 MVar load demand. The one line diagram of the above system and the corresponding power flows in it is shown in Figure 4, where the generators are located in different places and connected through the transmission lines. The MB-PSSs are installed at synchronous generator is given to MB-PSS as input whose output is used to get stable voltage (V_{pss}). The stable voltage is given generators to improve the transient performance after a big disturbance. The entire generator, units are equipped with the fast-acting static exciters and the speed governors. The rotor speed deviation of synchronous generator through the voltage regulator and exciter. The output voltage of the exciter is given to excitation system stabilizer and is compared with reference to terminal voltage. The output power from the

synchronous generator is given to infinite bus through transmission voltage. To analyze the performance of the MB-PSS, a model is developed in Simulink block set of MATLAB. The functional block set of MB-PSS is developed in Simulink environment which is given in Fig. 5.

7 Simulation Results and Discussion

The performance of RLS based PID with MB-PSS and SPARLS based PID with MB-PSS were studied in the Simulink environment for different operating conditions and the following test cases were considered for simulations.

- Case I: To normal load the variation of speed deviation, field voltage and load angle were analyzed for MB-PSS, without the MB-PSS, RLS & SPARLS based MB-PSS and RLS & SPARLS based PID with MB-PSS.
- Case II: The variation of the above mentioned cases were analyzed when system subjected to 150 % increased in loading condition.
- Case III: System was subjected to fault condition when the variation of the above mentioned cases were analyzed.

To illustrate the effectiveness and robustness of the proposed algorithm different possible case studies are explained as follows, the controller reduces the overshoot and settling time to the nominal level when subjected to MB-PSS, without the MB-PSS, RLS & SPARLS based MB-PSS and RLS & SPARLS based PID with MB-PSS and the inference of the simulation results are as follows.

Base Load Condition- Here, the synchronous machine subjected to base load is taken as 315 MW. The MB-PSS is installed in the corresponding exciter loop of all the generators and the performance characteristics is given in Figure 7 to 12. The performance of MB-PSS was demonstrated on a three machine nine bus systems in the Simulink environment for different operating conditions. Based upon the RLS and SPARLS algorithm MB-PSS based PID gain values are tuned in Matlab Simulink. From the Figure 8 it is observed that the SPARLS based PID with MB-PSS can provide, the better damping characteristic than the RLS based PID with MB-PSS. The SPARLS based PID with MB-PSS reduced the overshoot and the system reaches the steady state quickly compared with RLS based PID with MB-PSS. The speed deviation of the RLS & SPARLS based PID with MB-PSS are

shown in Figure 7 and Figure 8 which depicts that the SPARLS based PID with MB-PSS can provide the better damping characteristic than the RLS based PID with MB-PSS. From the Figure 8, it is observed that the RLS based PID with MB-PSS controller also gives better settling time (3.5 Sec). The SPARLS based PID with MB-PSS further reduces the settling time at 2 Sec and also the overshoot. By this effect, the field voltage (Figure 9) will be stable and in turn ensures the system stability. In response of Speed deviation Figure 8, the overshoot reduced to 0.015 from 0.013 using SPARLS based PID with MB-PSS therefore the system reaches the stable state quickly. It is necessary to maintain the speed in the synchronous generator should be making the system reach the steady state as early as possible for that SPARLS based PID with MB-PSS give better optimal solution compared to others. Normally for the smart system the load angle should be maintained around 15 to 45 degrees. Here it is inferred that after the inclusion of SPARLS based PID with MB-PSS the damping oscillation was reduced, it also boosts up the load angle 20 degrees. According to Figure 10, SPARLS based PID with MB-PSS improves the rotor angle to the maximum extent by reaching the settling time before 3 Sec. The performance of SPARLS and RLS in speed deviation is shown in Figure 11. From the results obtained, it is obvious that the speed estimated from the SPARLS tracks closely than actual speed even when there is a change in the parameter. The error in the speed estimation is almost negligible whereas RLS is not closer to the actual speed and fails to control the error in the speed estimator. The SPARLS based speed estimation is shown to overcome the RLS. The error of SPARLS and RLS (Figure 11 and Figure 12) are 0.2 % and 5 % respectively.

Increasing in Load Condition- In this case, the Synchronous generator is subjected to increased in a load of 50% from the base load. The performance characteristics of the system with SPARLS based PID with MB-PSS and RLS based PID with MB-PSS are illustrated from Figure 13 to 16. From the base load condition, it is observed that SPARLS based PID with MB-PSS performance is better than the other controller, in this increasing in load condition compared to the RLS & SPARLS are compared based on PID with MB-PSS alone. From the Figure 13, the SPARLS based PID with MB-PSS provides a better solution by reducing overshoot to 75% and the settling time in 2.5 Sec even in heavy load condition. By this effect the field voltage (Figure 15) will be stable and it will maintain the system stability. According to Figure 13, the overshoot was heavy for RLS based PID with MB-

PSS and it affects the stability of the system. The SPARLS based PID with MB-PSS reduces the overshoot and makes the system to reach steady state before 2.5 Sec. Therefore, it is inferred that SPARLS based PID with MB-PSS supports the synchronous generator to maintain synchronous speed even in increasing load condition. During the load condition, the SPARLS based PID with MB-PSS makes the system to settle in 2 Sec and it boosts up the system to maintain the field voltage (Figure 15). In this case, IT IS ALSO maintains stability IN the proposed system. To analyze the performance of RLS and SPARLS the speed deviation estimated for the increasing load condition is shown in Figure 13. The error estimated from RLS and SPARLS is shown in Figure 16 (b). From the results obtained, it is clearly understood that speed deviation estimated from the SPARLS is very well, even with the increasing load, the error is 0.45 %. Thus RLS based speed deviation is found to be less sensitive even in increasing load condition, this is because the RLS algorithm does not force any restriction on the input data formation, whereas speed deviation from the RLS deviated from the actual. It is also noted that the error in the speed deviation keeps on increasing. Thus, from the above analysis, it is understood that SPARLS algorithm exhibits stable performance, whereas RLS algorithm shows (Figure17) unstable performance. For the comparison, both the figures are shown with the same scale. From the results obtained, it is seen that the SPARLS based speed deviation displays stable performance that tracks the actual speed well whereas RLS becomes unstable and fails to reduce error. The SPARLS based speed deviation is shown to overcome the RLS based speed deviation.

Fault Condition- This illustrates the stability of the system during vulnerable condition, three phase fault is assumed to happen at the transmission line. The fault persists in the system for 0.01 Sec and it is cleared after 0.1 Sec. The parameters of the system during fault condition are illustrated in Figure 18 to Figure 19. From the Figure 18, it is observed that the RLS based PID with MB-PSS produced more overshoot and settles at 5 Sec. The SPARLS based PID with MB-PSS reduces the settling time of 3.5 Sec and also the overshoot. According to Figure18, the overshoot was high for RLS based PID with MB-PSS, therefore, the stability of the system was affected. The SPARLS based PID with MB-PSS reduces the overshoot to 50% and makes the system to reach steady state before 3.5 Sec. From this case, it is inferred that PID with MB-PSS supports the synchronous generator to maintain synchronous speed even at severe fault

condition.

8 CONCLUSION

This paper proposes a novel SPARLS algorithm developed for tuning of MB-PSS based PID. The SPARLS algorithm is simple to understand and easier to design. The proposed SPARLS algorithm is developed to tune the parameter of PSS based PID and its performance is compared with RLS for the various cases such as base load, increasing in load and fault conditions. Through extensive simulations, the proposed SPARLS is shown to improve the PSS based PID parameters as compared to RLS. The proposed method is compared with the conventional RLS algorithm. The error in the speed deviation from the SPARLS algorithm under base and increasing in load condition is found to be 0.2% and 0.45 % respectively. The SPARLS algorithm is performing very well than the conventional RLS algorithm. The error in the speed deviation through the proposed SPARLS algorithm under base and increasing in load condition is found to be 0.2%. It is concluded that the proposed SPARLS algorithm provides a better results, less complex and better performance than that conventional RLS algorithm over a wide operating range.

References:

- [1] Larsen, E. V., and Swann, D. A. "Applying power system stabilizers parts III," IEEE Trans. Power App. Syst., Vol. 100, No. 6, (1981) pp. 3017-3046.
- [2] M. Mary Linda, N. Kesavan Nair, "Optimal Design of Fuzzy Based Power System Stabilizer Self Tuned by Robust Search Algorithm," Journal of Computing, Vol. 1, No. 1, (2009) pp. 44-48.
- [3] Neeraj Gupta and Sanjay K. Jain, "Comparative Analysis of Fuzzy Power System Stabilizer Using Different Membership Functions," International Journal of Computer and Electrical Engineering, Vol. 2, No. 2, (2010) pp. 262-267.
- [4] K. Sundareswaran and S. Razia Begum, "Genetic tuning of a power system stabilizer", European Transactions on Electrical Power, Vol. 14, No. 3, (2004)pp 151160.
- [5] Y. Zhang G. P. Chen 0. P. Malik G. S. Hope, "An Artificial Neural Network based Adaptive Power System Stabilizer," IEEE Transactions on Energy Conversion, Vol. 8, No. 1, (1993)pp. 71-77.

- [6] Boonserm Changaroon, Suresh Chandra Srivastava and Dhadbanjan Thukaram, "A Neural Network Based Power System Stabilizer Suitable for On-Line Training A Practical Case Study for EGAT System," IEEE Transactions on Energy Conversion, Vol. 15, No. 1, (2000) pp. 103-109.
- [7] Miguel Ramirez-Gonzalez, and O. P. Malik, "Power System Stabilizer Design Using an Online Adaptive Neuro-fuzzy Controller With Adaptive Input Link Weights," IEEE Transactions on Energy Conversion, Vol. 23, No. 3, (2008) pp. 914-922.
- [8] Ramos, R.A., Alberto, L.F.C., and Bretas, N.G, "A new methodology for the coordinated design of robust decentralized power system damping controllers," IEEE Transactions on Power Systems, Vol. 19, No. 1, (2004) pp. 444-454.
- [9] Meng Yue, and Robert A. Schlueter, "Synthesis Power System Stabilizer Design Using a Bifurcation Subsystem Based Methodology," IEEE Transactions on Power Systems, Vol. 18, No. 4, (2003) pp. 1497-1506.
- [10] Amitava Sil, T. K. Gangopadhyay, S. Paul and A. K. Maitra, "Design of Robust Power System Stabilizer Using H Mixed Sensitivity Technique," Third International Conference on Power Systems, Kharagpur, INDIA, December 27-29, (2009).
- [11] Ruhua You, Hassan J. Eghbali, and M. Hashem Nehrir, "An Online Adaptive Neuro-Fuzzy Power System Stabilizer for Multimachine Systems," IEEE Transactions on Energy Conversion, Vol.18, No.1, (2003) pp. 128-135.
- [12] Wenxin Liu, Ganesh K. Venayagamoorthy, and Donald C. Wunsch, "Design of an adaptive neural network based power system stabilizer," Elsevier Science, (2003) pp. 891-899.
- [13] K.R.Sudha, Y.Butchi Raju and Prasad Reddy.P.V.G.D, "Adaptive Power System Stabilizer using support Vector Machine," International Journal of Engineering Science and Technology, Vol. 2, No. 3, (2010) pp. 442-447.
- [14] N.M. Tabatabaei, M. Shokouhian Rad, "Designing Power System Stabilizer with PID Controller," International Journal on Technical and Physical Problems of Engineering (IJTPE), Vol. 2, No. 3, (2010) pp. 1-7.
- [15] Sayed Mojtaba Shirvani Boroujeni, Reza Hemmati, Hamideh Delafkar and Amin Safarnezhad Boroujeni, "Optimal PID power system stabilizer tuning based on particle swarm optimization," Indian Journal of Science and Technology, Vol. 4, No. 4, (2011) pp. 379-384.
- [16] Rabih A. Jabr, Bikash C. Pal, and Nelson Martins, "A Sequential Conic Programming Approach for the Coordinated and Robust Design of Power System Stabilizers," IEEE Transactions on Power Systems, Vol. 25, No. 3, (2010) pp. 1627-1637.
- [17] Hasan Fayazi Boroujeni, Sayed Mojtaba Shirvani Boroujeni and Reza Hemmati, "Robust PID power system stabilizer design based on pole placement and nonlinear programming methods," Indian Journal of Science and Technology, Vol. 4, No. 4, (2011) pp. 456-463.
- [18] Soheil Ganjefar, Mojtaba Alizadeh, "On-line self-learning PID based PSS using self-recurrent wavelet neural network identifier and chaotic optimization," COMPEL: The International Journal for Computation and Mathematics in Electrical and Electronic Engineering, Vol. 31, No. 3, (2012) pp. 1872-1891.
- [19] Galotto. L, Pinto. JOP, Filho J. A. B and Lambect- Torres, "Recursive least square and genetic algorithm based tool for PID controllers tuning," IEEE conference on Intelligent information technology application, Vol. 3, (2008) pp. 584-600.
- [20] Daniele Angelosante, Juan Andrs Bazerque, and Georgios B. Giannakis, "Online Adaptive Estimation of Sparse Signals: Where RLS Meets the L1-Norm," IEEE Transactions on Signal Processing, Vol. 58, No. 7, (2010) pp. 3436-3447.
- [21] Balwinder Singh Surjan, Ruchira Garg, "Power System Stabilizer Controller Design for SMIB Stability Study," International Journal of Engineering and Advanced Technology (IJEAT), Vol. 2, No. 1, (2012) pp. 209-214.
- [22] Yuan- Yih Hsu, Kan-Lee Liou, "Design of Self-Tuning PID Power System Stabilizers for Synchronous Generators," IEEE Transactions on Energy Conversion, Vol. EC-2, No. 3, (1987) pp. 343-348.

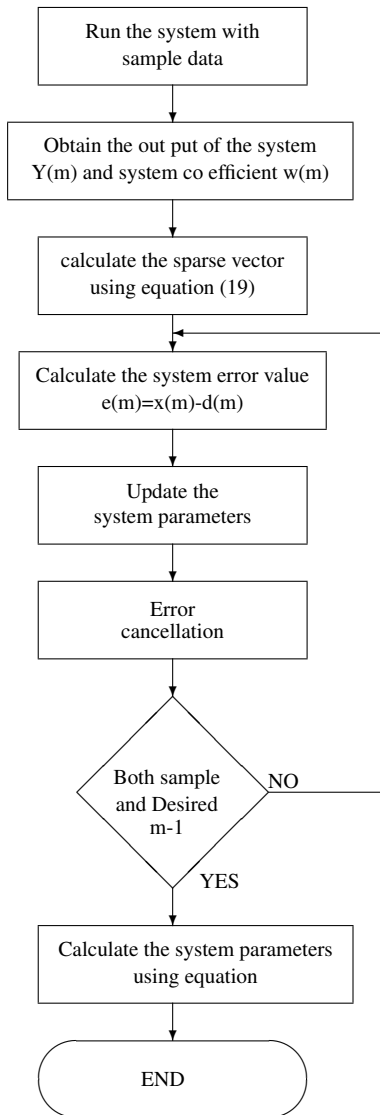


Figure 4: This is my flow chart

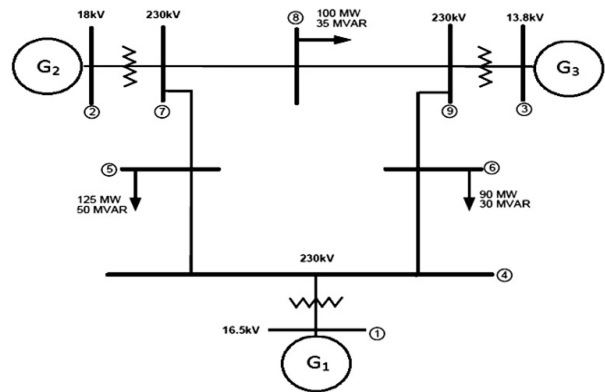


Figure 5: One line diagram Three Machines, Nine Bus system

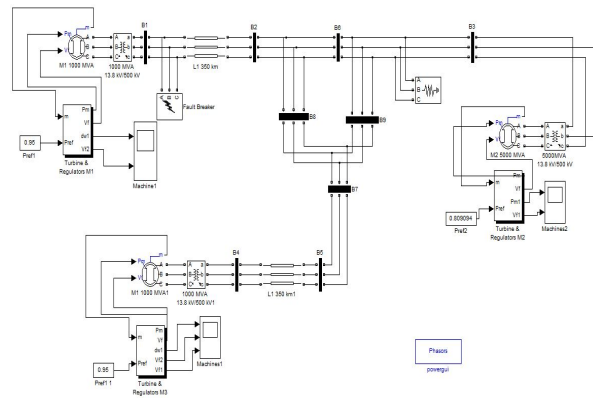


Figure 6: Simulink diagram

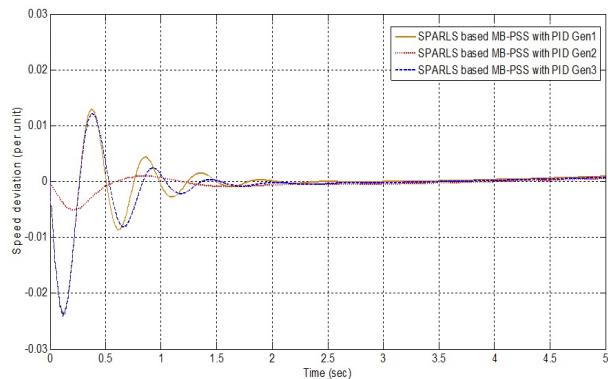


Figure 7: Speed deviation during a base load condition

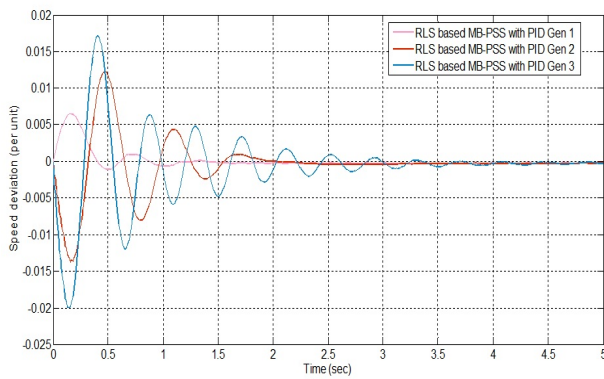


Figure 8: Speed deviation during a base load condition

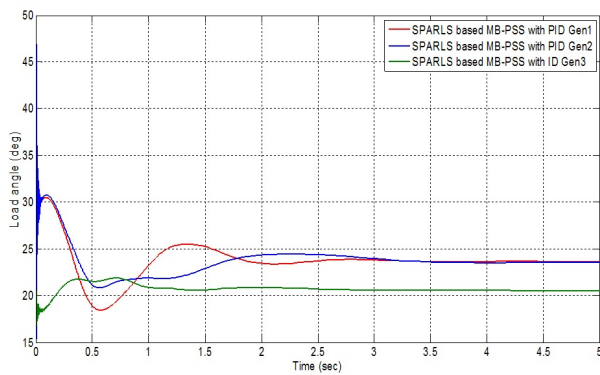


Figure 9: Field voltage during base load condition

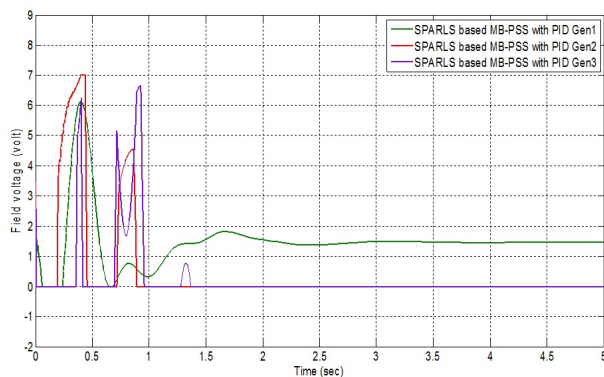
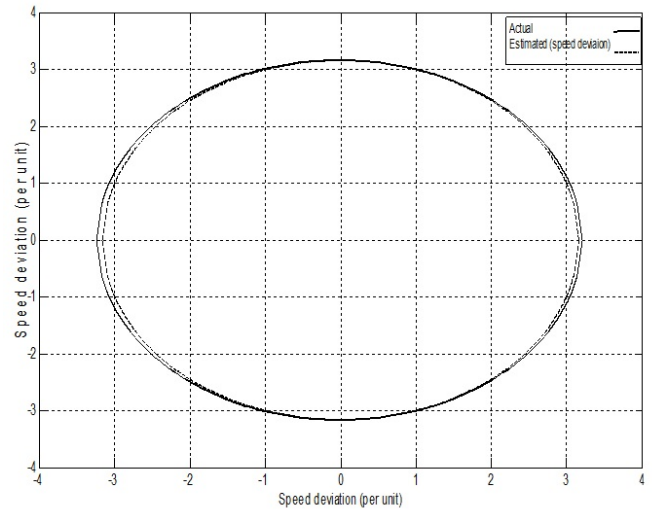
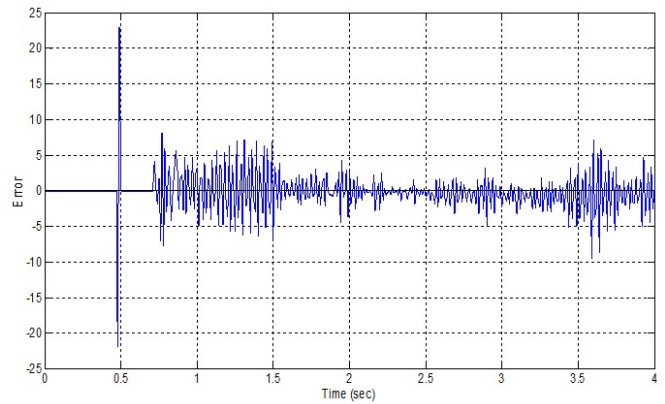


Figure 10: Load angle during base load condition

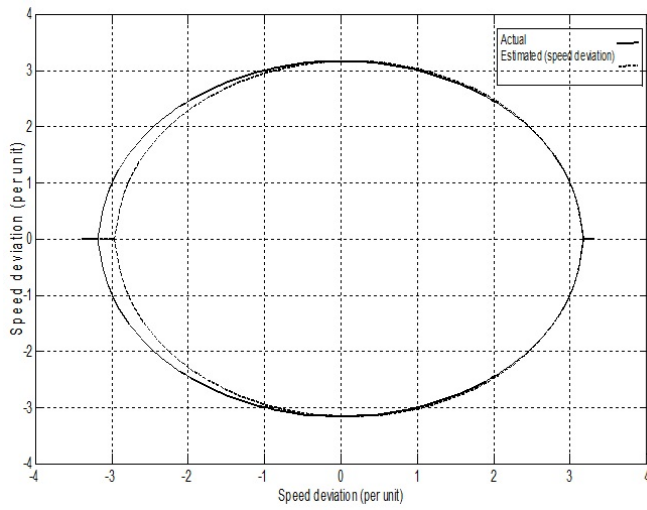


(a)

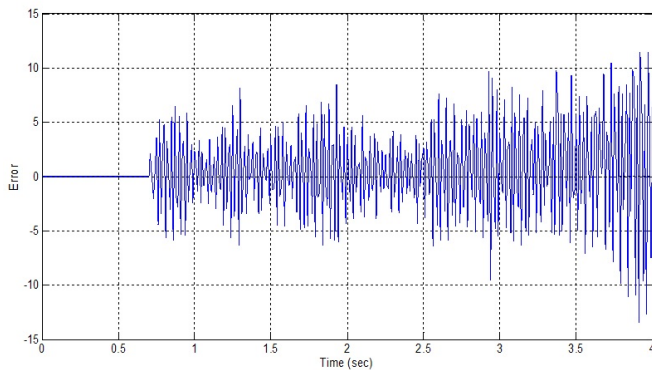


(b)

Figure 11: SPARLS (a) Performance curves for base load condition: Actual and estimated speed deviation (b) Performance curves for base load condition: error between actual and estimated



(a)



(b)

Figure 12: RLS (a) Performance curves for base load condition: Actual and estimated speed deviation (b) Performance curves for base load condition: error between actual and estimated

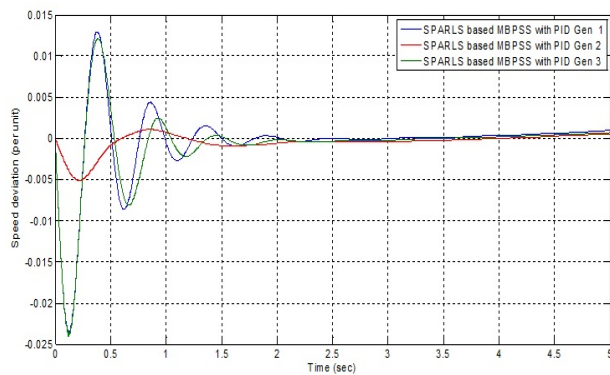


Figure 13: Speed deviation during increased load condition

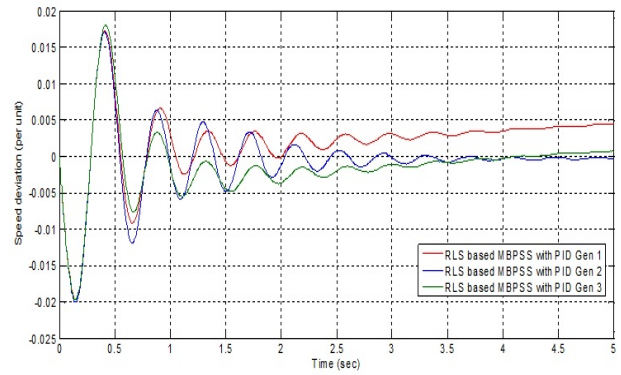


Figure 14: Speed deviation during increased load condition

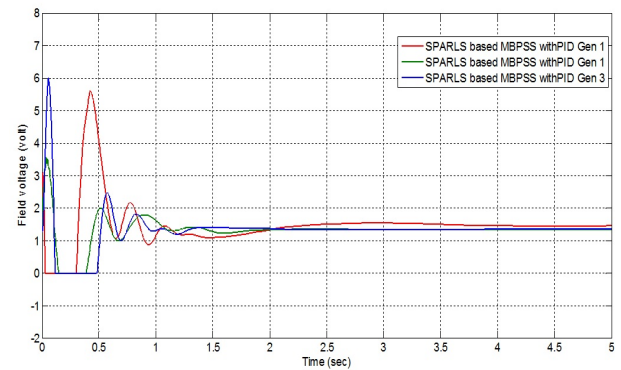
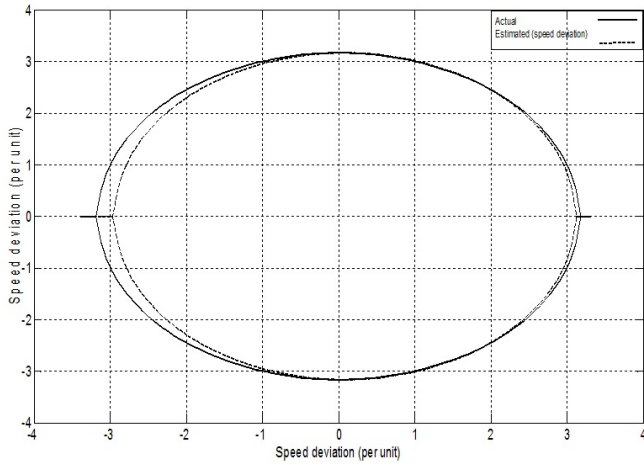
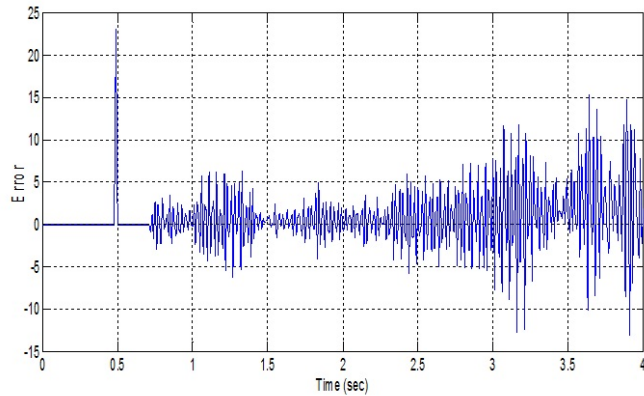


Figure 15: Field voltage during increased load condition

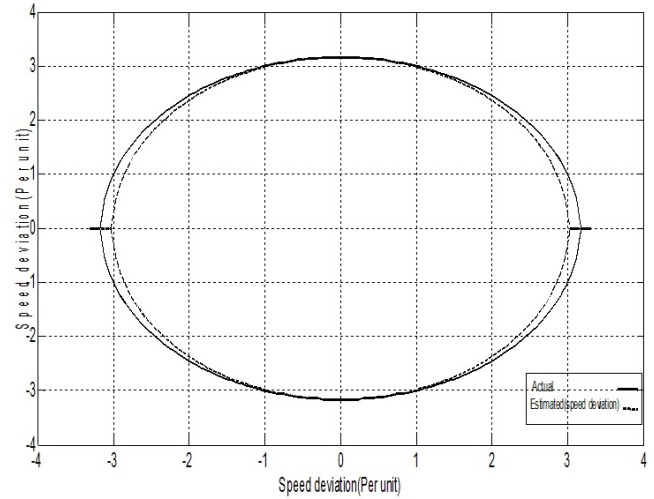


(a)

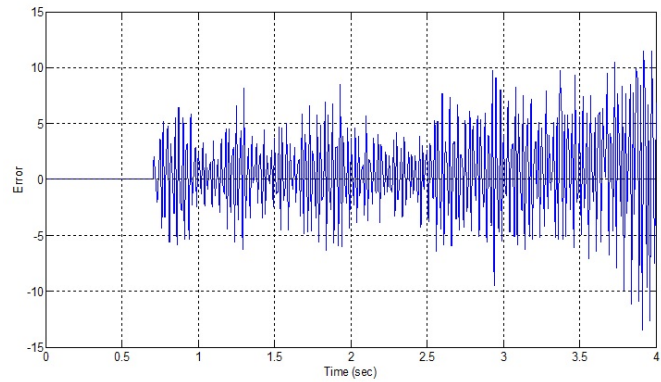


(b)

Figure 16: (a) Performance curves for increased load condition: Actual and estimated speed deviation (SPARLS). (b) Performance curves for increased load condition: error between actual and estimated (SPARLS).



(a)



(b)

Figure 17: (RLS). (a) Performance curves for increased in load condition: Actual and estimated speed deviation. (b) Performance curves for increased load condition: error between actual and estimated.

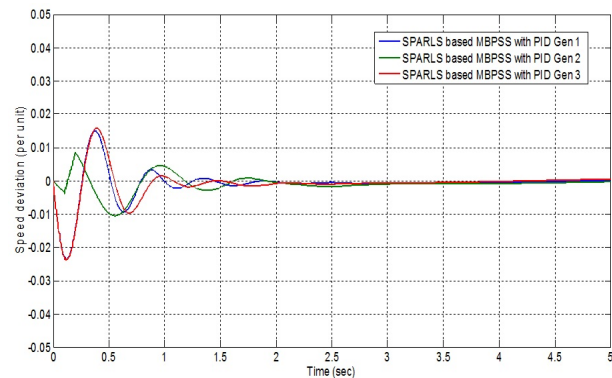


Figure 18: Speed deviation during fault condition
 Volume 2, 2017

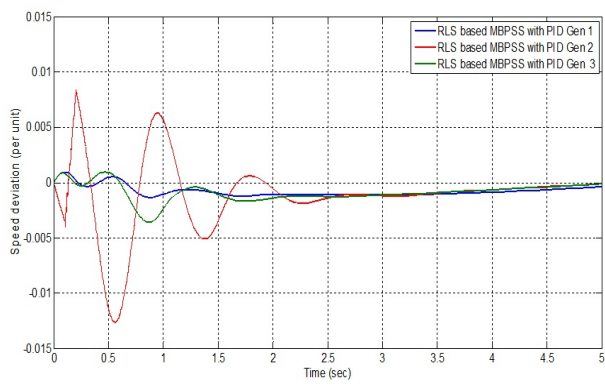


Figure 19: Speed deviation during fault condition